Comparison between Full Wave and Ray-Tracing Calculations to Examine Scenarios for Electron Bernstein Wave Heating in LHD*)

Hiroe IGAMI, Atsushi FUKUYAMA[1)], Hiroshi IDEI[2)], Kazunobu NAGASAKI[3)], Yuki GOTO[4)], Shin KUBO, Takashi SHIMOZUMA, Yasuo YOSHIMURA, Hiromi TAKAHASHI, Toru I. TSUJIMURA and Ryohei MAKINO

National Institute for Fusion Science, 322-6 Oroshi-cho Toki 509-5292, Japan
[1)]*Department of Nuclear Engineering, Kyoto University, Nishikyo-ku, Kyoto 615-8530, Japan*
[2)]*Research Institute for Applied Mechanics, Kyushu University, 6-1 Kasuga-koen, Kasuga 816-8580, Japan*
[3)]*Institute of Advanced Energy, Kyoto University, Uji 611-0011, Japan*
[4)]*Department of Energy Engineering and Science, Nagoya University, Furo-cho, Chikusa-ku, Nagoya 464-8603, Japan*

(Received 30 November 2015 / Accepted 18 April 2016)

With the use of the density scale length and the magnetic field strength around the O-X mode conversion region in the LHD for 77 GHz EC waves, the full wave calculations by the TASK/WF2D code have been performed. The wave patterns obtained by full wave calculation have been compared with the trajectories obtained by multi ray tracing calculations. For the X-mode and the O-mode reflected near each cutoff, wave patterns obtained by full wave calculations and trajectories obtained by multi ray-tracing correspond to each other well. On the contrary, trajectories of the rays restarted at the high field side of the evanescent region between the plasma and the left handed cutoffs do not cover fully the wave patterns after the O-X mode conversion obtained by full wave calculations. Improvement of the manner to restart the ray-tracing is required. This improvement can provide a more precise view of the propagation of the EBWs and may contribute to examining scenarios for electron Bernstein wave heating.

Keywords: electron cyclotron resonance heating, electron Bernstein wave, full wave calculation, ray-tracing

DOI: 10.1585/pfr.11.2403098

1. Introduction

Electron cyclotron resonance heating and current drive (ECRH and ECCD) in over dense plasmas where the electron density is more than the cutoff density of the electron cyclotron (EC) wave are available with use of the electron Bernstein waves (EBWs). Since the EBWs are the electrostatic waves, they should be excited via the linear mode conversion process inside the plasma by launching the electromagnetic (EM) waves from the vacuum region [1]. To excite the EBWs efficiently when the density scale length in the "mode conversion region" is long enough compared to the wavelength, as in the over dense plasma generated in the Large helical device (LHD), the EM waves should be injected with an appropriate polarization to couple with the O-mode at the plasma boundary toward an appropriate direction so that the parallel refractive index $N_{//}$ consists with [2] or is very close to the optimum value $N_{//\mathrm{opt}} = \sqrt{\Omega_{\mathrm{ce}}/(\omega + \Omega_{\mathrm{ce}})}$ at the plasma cutoff (PC), where Ω_{ce} is the cyclotron angular frequency and ω is the wave angular frequency. The injected O-mode couples with the X-mode that propagates toward the upper hybrid resonance (UHR) and finally couples with the EBW.

author's e-mail: igami@LHD.nifs.ac.jp

*) This article is based on the presentation at the 25th International Toki Conference (ITC25).

In the LHD, ECRH in over dense plasmas by EBWs excited via the O-X-EBW mode conversion process mentioned above was performed [3]. In the analyses of the EBW heating experiment, the multi ray-tracing taking into account the finite beam width is used. However, the ray-tracing cannot provide a precise view of the wave propagation around the mode conversion region because the WKB approximation is not valid there. When $N_{//}$ is not strictly equal to $N_{//\mathrm{opt}}$ at the PC the ray-tracing shows that the injected O-mode is just reflected in front of the evanescent region even if a part of the power of the injected O-mode can tunnel through the evanescent region between the PC and the left handed cutoff (LC) and can couple with the X-mode with the efficiency as the analytic form written below suggests [4].

$$T_{\mathrm{OX}} = \exp\{-\pi k_0 L_{\mathrm{n}} (\beta/2)^{1/2} \times [2(1+\beta)(N_{//} - N_{//\mathrm{opt}})^2 + N_{\mathrm{v}}^2]\}, \quad (1)$$

where $k_0 = \omega/c$, c is the velocity of light in vacuum, L_{n} is the scale length of the density gradient, N_{v} is the refractive index perpendicular to the magnetic field and the density gradient.

To investigate the wave propagation and absorption after the tunneling through the evanescent region, an "expe-

dient manner" to restart the ray-tracing calculation at the edge of the higher density side of the evanescent region has been used to analyze the wave propagation in the overdense region [5]. However, to describe the wave propagation around the mode conversion region precisely the full wave analysis that solves the Maxwell's equation directly is required with taking into account the non-uniform plasma profiles and the distribution of the wave electric field. We are developing a numerical code including the TASK/WF2D code that solves the Maxwell's equation by finite elements method (FEM) in two-dimensional space [6]. This numerical code can describe the wave propagation across the evanescent region with taking into account the non-uniform plasma profiles and arbitrary distribution of the electric field of the incident wave. In this paper, comparisons between the full wave calculations obtained by the TASK/WF2D code around the evanescent region and the ray-tracing calculations with use of the "expedient manner" to check its validity is reported. In section 2, the systems for the full wave calculations (TASK/WF2D) and the ray-tracing calculations are explained. In section 3, comparison of the calculation results by full wave and ray-tracing calculations with use of the parameters around the O-X mode conversion region in LHD are shown. In section 4, we summarize the contents.

2. Systems for the Full Wave and Ray-Tracing Calculations

TASK/WF2D solves the wave equation as the boundary problem

$$\nabla \times \nabla \times \boldsymbol{E} - \boldsymbol{k}_0^2 \quad \boldsymbol{\varepsilon} \cdot \boldsymbol{E} = i\omega\mu_0 \boldsymbol{j}_{\mathrm{ext}}, \tag{2}$$

where $\boldsymbol{\varepsilon}$ is the dielectric tensor, $\boldsymbol{E}$ is the electric field vector, $\boldsymbol{\mu}_0$ is the vacuum permeability, $\boldsymbol{j}_{\mathrm{ext}}$ is the external current vector. Figure 1 shows a schematic view of the system of TASK/WF2D used in the analysis here. The calculation area is defined with input parameters x_{c}, x_{w}, z_{min}, and z_{max}. The electric field is calculated at each meshed position along the x and the z directions. The boundary value of the electric field is given at $x = x_{\mathrm{w}}$. In the current version of TASK/WF2D, plasma parameters that change linearly along the z and x directions can be given. The permittivity tensor of the collisional cold plasma is used. The electric field as the boundary value is given based on the electric field at the aperture plane of the rectangular waveguide whose inner width is a. At the aperture, the electric field strength is given as the basic rectangular waveguide mode $E = E_0 \sin(\pi l/a)$, where l is the distance from (x_{w}, z_1) along the z' direction shown in Fig. 1 and a is the length of the inner side of the waveguide. When the injection angle between the wave vector and the z direction is θ, the electric field strength along the z direction at $x = x_{\mathrm{w}}$ is given with taking into account the phase delay of the plane wave front so that the phases ϕ_1 at (x_{w}, z_1) and ϕ_2 at (x_{w}, z_2) should be set as input parameters so that $d\phi = \phi_2 - \phi_1 = k_0(z_2 - z_1)\cos\theta$. In the region $z_1 \le z \le z_2$ at $x = x_{\mathrm{w}}$ the y and the z components of the electric field are given as $E_y = E(\sin\psi - ie\cos\psi)$, and $E_z = E(\cos\psi + ie\sin\psi)$ with use of real value input parameters E, e, and ψ to determine relative electric field strength and phase. To show the wave propagation across the evanescent region clearly without the reflection at the conductive wall, the wave absorber whose thickness is w_{damp} given as an input parameter can be put in along the calculation boundary without the region between $(x_{\mathrm{w}}, z_{\mathrm{dmin}})$ and $(x_{\mathrm{w}}, z_{\mathrm{dmax}})$. Here z_{dmin} and z_{dmax} are given as input parameters.

In the ray-tracing calculations, the same magnetic field and the electron density profile as used in the full wave calculations by the TASK/WF2D code are adopted. The dispersion equation of the cold collisionless plasma

$$aN_\perp^4 - bN_\perp^2 + c = 0 \tag{3}$$

is used, where $a = S$, $b = RL + PS - (P + S)N_{//}^2$, $c = P(R - N_{//}^2)(L - N_{//}^2)$, $S = 1 - \alpha/(1+\beta^2)$, $R = 1 - \alpha/(1-\beta)$, $L = 1 - \alpha/(1+\beta)$, $P = 1 - \alpha$, $\alpha = (\omega_{\mathrm{p}}/\omega)^2$, $\beta = \Omega_{\mathrm{ce}}/\omega$, ω_{p} is the plasma angular frequency. As mentioned in section 1, an "expedient manner" is used to restart the ray-

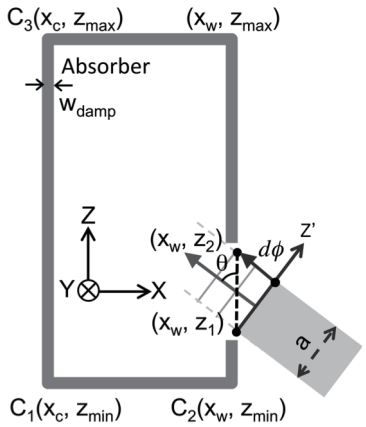

Fig. 1 Schematic view of calculation system for TASK/WF2D.

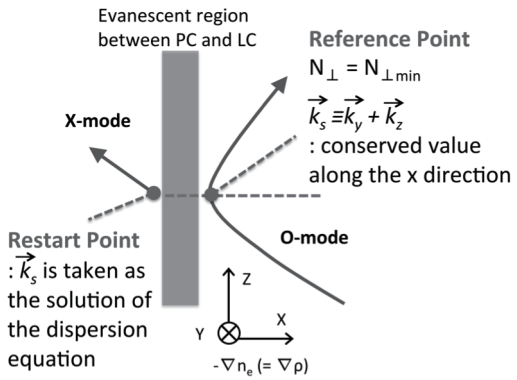

Fig. 2 Schematic view of the "expedient manner" to restart the ray-tracing at the high field side across the evanescent region.

tracing after the O-mode tunnels through the evanescent region and couples with the X-mode in the high density side. Figure 2 shows the schematic view of the "expedient manner". When the injected O-mode is reflected near the evanescent region between the PC and the LC, we determine the reference point where the perpendicular component of the refractive index $N_\perp$ becomes the minimum. The wave vector at the reference point is taken to be a conserved value $\boldsymbol{k}_s$ and look for the point where $\boldsymbol{k}_s$ is the solution of eq. (3) at the high density side across the evanescent region along the direction of the density gradient.

3. Comparison of the Calculation Results by Full Wave and Ray-Tracing Calculations

In the calculations, the wave frequency 77 GHz that is used for ECRH in the LHD is selected. Since the typical density scale length normalized by the vacuum wavelength of the 77 GHz EC wave $L_n/\lambda_0 = 53$ and $\beta = \Omega_{ce}/\omega = 0.615$ at the plasma cutoff in discharges when the ECRH by EBWs excited via the O-X-EBW mode conversion is performed, we adopt a simple linear electron density profile changes only along the x direction with $L_n/\lambda_0 = 53$ and a uniform magnetic field to be $\beta = 0.615$ parallel to the z direction. In TASK/WF2D calculation, we assume the case where the length of the inner side of the waveguide, $a = 0.1$ m. The selected mesh spacing of the full wave calculation is 4 mm.

Note that in the real LHD configuration, the electron density and magnetic field change three-dimensionally and the EM waves are launched as a Gaussian beam. However, it is worth to examining the propagation of the waves that have a finite beam width to verify the validity of the "expedient manner" to restart the ray-tracing.

Figure 3 shows a wave pattern as a color map of the real x component of the electric field strength and a distribution map of the absorbed power by collisional damping as a gray-scaled image near the O-X mode conversion region when the O-mode dominant EM waves are injected with the injection angle $\theta_{inj} = \theta_{opt} = \arccos(N_{//opt})$ from lower right side. A part of the injected EM waves reaches the high density side of the PC and propagates backward toward the UHR. The distribution of the absorbed power suggests this backward wave is fully absorbed by collisional damping near the UHR. Although the launching angle θ_{inj}, is set to be θ_{opt}, split wave patterns that might be reflected as the O-mode near the PC are shown. Since the radiation pattern of the waves launched from the waveguide aperture is not strictly the same as that of the plane waves, the broadening of the wave pattern might cause deviation of $N_{//}$ from $N_{//opt}$ and reflection near the PC.

With taking into account the broadening of the launched wave we performed multi ray-tracing calculations with $\theta_{inj} = \theta_{opt}$ at the beam center, $\theta_{inj} = \theta_{opt} \pm 1.5$ degrees at each edge of the beam, and plotted the trajectories over the wave patterns in Fig. 4, where the real x, y, z components of the electric field strength are shown as color maps. Trajectories of the O-mode reflected near the PC are plotted except the central ray of $N_{//} = N_{//opt}$. Trajectories of the reflected O-mode whose $N_{//}$ deviates from $N_{//opt}$ a little, well correspond to the split wave pattern of the reflected O-mode mentioned above. Wave patterns that might correspond to the X-mode reflected near the RC are also shown. The multi-ray trajectories of the reflected X-mode correspond well to the wave patterns. On the other hand the trajectories of the rays restarted with the "expedient manner" explained in Fig. 2 do not fully cover the wave patterns of the backward waves after the O-X mode conversion that is obtained from TASK/WF2D calculation.

For the cases of $N_{//} = N_{//opt} + 0.02$ and $N_{//} = N_{//opt} + 0.1$, full wave and multi ray tracing calculations were per-

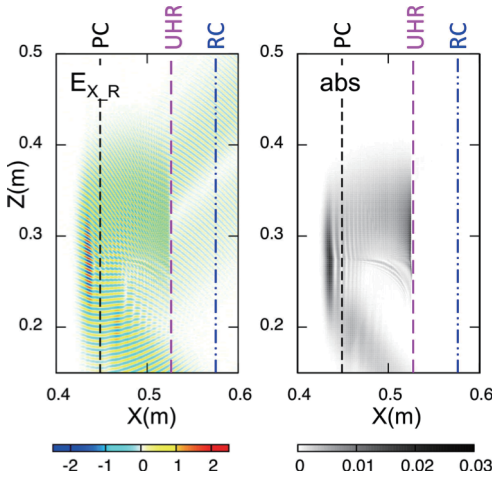

Fig. 3 Color map of the real x component of the electric field strength (left) and gray-scaled image of the absorbed power by collisional damping (right) when $\theta_{inj} = \theta_{opt}$.

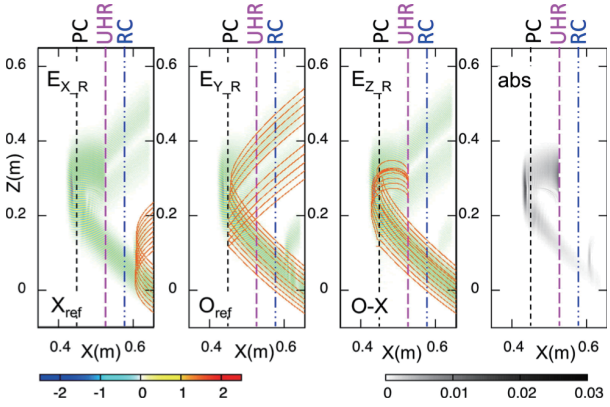

Fig. 4 (From the left) color maps of the real x, y, z components of the electric field strength and gray-scaled image of the absorbed power when $\theta_{inj} = \theta_{opt}$. Multi ray trajectories of the reflected X-mode, reflected O-mode, and mode converted X-mode are plotted over the maps. At beam center $\theta_{inj} = \theta_{opt}$, and at each edge of the beam $\theta_{inj} = \theta_{opt} \pm 1.5$.

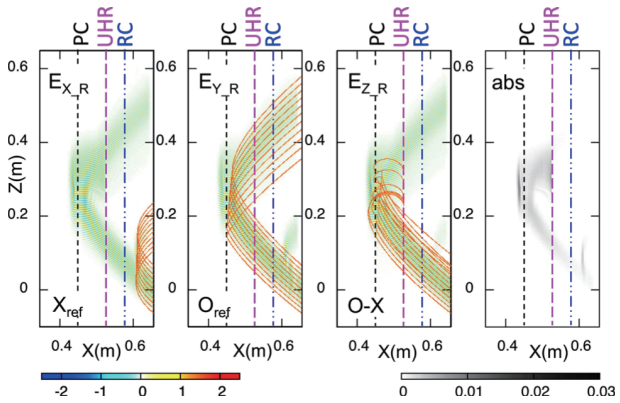

Fig. 5 Similar plots to Fig. 4 when $\theta_{inj} = \arccos(N_{//opt} + 0.02)$.

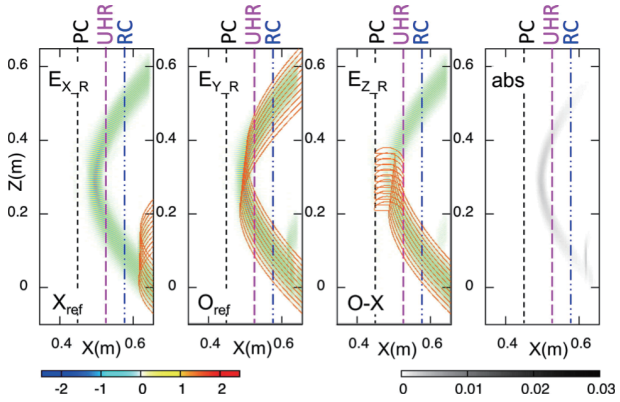

Fig. 6 Similar plots to Fig. 4. when $\theta_{inj} = \arccos(N_{//opt} + 0.1)$.

formed in the same manner. As shown in Fig. 5, the deviation of $N_{//}$ from $N_{//opt}$ by 0.02 allows efficient O-X mode conversion while the deviation of $N_{//}$ from $N_{//opt}$ by 0.1 allows a very poor O-X mode conversion rate as shown in Fig. 6. Trajectories of the ray of the reflected waves with taking into account the beam broadening also correspond well to the wave pattern obtained by full wave calculations in these cases. Since the $N_{//}$ at the beam center deviates from $N_{//opt}$ the reflection of the O-mode occurs at the beam center and the wave patterns are not split as in the case of $N_{//} = N_{//opt}$. Trajectories of the rays after the O-X mode conversion do not cover the wave patterns obtained by full wave calculations fully also.

As explained in Fig. 2, the restart point of the ray-tracing is determined as a point shifted along the density gradient (the x direction in this case) from the reference point. However, the full wave calculations suggest the tunneling waves actually proceed obliquely upward. It might be better to place the restart point with taking into account the propagation toward the direction perpendicular to the direction of the density gradient (the z direction in this case) as shown in Fig. 7. However, verifications with the full wave and ray tracing calculations are required for how

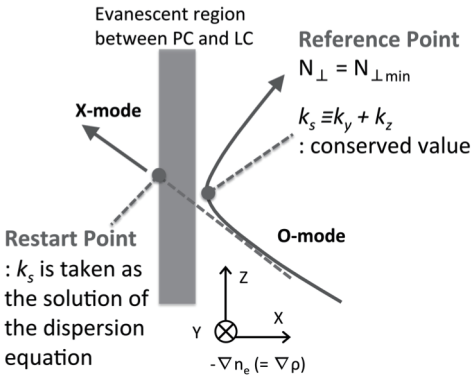

Fig. 7 Schematic view of the improved idea of the "expedient manner" to restart the ray-tracing.

to take the appropriate domain of the asymptotic line of the trajectory drawn in Fig. 7.

4. Summary

For the analysis of the ECRH by EBWs excited via the O-X-EBW mode conversion process performed in the LHD, a numerical code including the TASK/WF2D code is under development. As the first step, full wave calculations by TASK/WF2D with the use of the density scale length and the magnetic field strength around the O-X mode conversion region in the LHD for 77 GHz EC waves have been performed and compared with the multi ray tracing calculations. For the O-mode and X-mode reflected near their cutoffs, the wave patterns obtained by full wave calculations and the trajectories obtained by multi ray-tracing calcuations correspond to each other well if the broadening of the injected beam is taken into account. On the other hand trajectories of the multi rays after the O-X mode conversion do not cover the wave patterns fully. It has been suggested that it might be better to place the restart point with taking into account the propagation toward the direction perpendicular to the direction of the density gradient. Verifications with the full wave and ray tracing calculations will be required for the improvement of the "expedient manner" to determine the restart point. This improvement can provide a more precise view of the propagation of the EBWs and may contribute to examining scenarios for electron Bernstein wave heating.

[1] H.P. Laqua, Plasma Phys. Control. Fusion **49**, R1 (2007).
[2] J. Preinhaelter and V. Kopecky, J. Plasma Phys. **10**, 1 (1973).
[3] H. Igami *et al.*, Plasma Fusion Res. **7**, 2402110 (2012).
[4] E. Mjølhus, J. Plasma Phys. **31**, 7 (1984).
[5] H. Igami *et al.*, Plasma Sci. Technol. **11**, 430 (2009).
[6] A. Fukuyama, H. Igami and H. Idei, 41st European Physical Society Conference on Plasma Physics (EPS 2014) P4.014 (2014).